NeuroImage 232 (2021) 117909

Contents lists available at ScienceDirect

NeuroImage

journal homepage: www.elsevier.com/locate/neuroimage

Size constancy affects the perception and parietal neural representation of object size

Stephanie Kristensen[a], Alessio Fracasso[b,c], Serge O. Dumoulin[b,d,e], Jorge Almeida[a], Ben M. Harvey[d,*]

[a] Faculty of Psychology and Education Sciences, University of Coimbra, Rua do Colégio Novo, 3000-115 Coimbra, Portugal
[b] Spinoza Centre for Neuroimaging, Meibergdreef 75, 1105 BK Amsterdam, the Netherlands.
[c] Institute of Neuroscience and Psychology, University of Glasgow, 62 Hillhead Street, Glasgow G12 8QB, United Kingdom
[d] Experimental Psychology, Helmholtz Institute, Utrecht University, Heidelberglaan 1, Utrecht 3584 CS, the Netherlands
[e] Experimental and Applied Psychology, VU University Amsterdam, Van der Boechorststraat 1, Amsterdam 1081 BT, the Netherlands

ARTICLE INFO

Keywords:
Object size
Size constancy
Serial dependence
Functional MRI

ABSTRACT

Humans and animals rely on accurate object size perception to guide behavior. Object size is judged from visual input, but the relationship between an object's retinal size and its real-world size varies with distance. Humans perceive object sizes to be relatively constant when retinal size changes. Such size constancy compensates for the variable relationship between retinal size and real-world size, using the context of recent retinal sizes of the same object to bias perception towards its likely real-world size. We therefore hypothesized that object size perception may be affected by the range of recently viewed object sizes, attracting perceived object sizes towards recently viewed sizes. We demonstrate two systematic biases: a central tendency attracting perceived size towards the average size across all trials, and a serial dependence attracting perceived size towards the size presented on the previous trial. We recently described topographic object size maps in the human parietal cortex. We therefore hypothesized that neural representations of object size here would be attracted towards recently viewed sizes. We used ultra-high-field (7T) functional MRI and population receptive field modeling to compare object size representations measured with small (0.05–1.4°diameter) and large objects sizes (0.1–2.8°). We found that parietal object size preferences and tuning widths follow this presented range, but change less than presented object sizes. Therefore, perception and neural representation of object size are attracted towards recently viewed sizes. This context-dependent object size representation reveals effects on neural response preferences that may underlie context dependence of object size perception.

1. Introduction

Object size perception guides human and animal behavior and decisions, for example when planning to grasp an object or choosing the larger of two fruits. However, while object size is often determined visually, the relationship between an object's retinal size and its real-world size varies with distance. Indeed, an object appears larger when placed in part of a scene that appears further away, and the cortical activation the object produces is correspondingly larger, even with no binocular disparity cues to distance (Murray et al., 2006). This effect of spatial scene context is mirrored by a temporal size constancy effect: sequentially presented objects appeal closer in size than they are (Holway and Boring, 1941). These spatial and temporal size constancy effects are thought to compensate for changes in object size with distance, thereby biasing size estimates towards likely real-world sizes. Like considering the sizes of surrounding objects (spatial context), accounting for recently viewed object sizes (temporal context) could compensate for the variable relationship between retinal size and real-world size, when the object's real-world size is unknown or ambiguous.

In behavioral studies, perception of several stimulus properties has recently been shown to depend on the temporal context of recently presented stimuli, a phenomenon known as serial dependence (Cicchini et al., 2014; Fischer and Whitney, 2014; Liberman et al., 2014). Here, perception of currently presented stimuli is attracted towards the properties of recently presented stimuli, making them appear more alike than they are. Serial dependence is proposed to increase perceptual stability and reduce required neural processing by assuming that visual stimulus properties are likely to remain similar over short intervals. It appears to be pervasive throughout visual perception, affecting perception of low-level features such as orientation (Fischer and Whitney, 2014), high-level properties such as face identity (Liberman et al.,

* Corresponding author.
E-mail address: b.m.harvey@uu.nl (B.M. Harvey).

https://doi.org/10.1016/j.neuroimage.2021.117909
Received 7 July 2020; Received in revised form 30 November 2020; Accepted 23 February 2021
Available online 27 February 2021

2014), and quantities such as numerosity (Cicchini et al., 2014). Here we hypothesize that serial dependence may affect visual object size perception, helping compensate for the variable relationship between retinal size and real-world size.

We recently demonstrated selective neural responses to object size, organized into topographic maps in human parietal cortex (Harvey et al., 2015). These parietal areas are thought to link visual processing to action planning (Ferri et al., 2015; Orban and Caruana, 2014). Their responses may be affected by modulatory influences like attention (Silver et al., 2005), allowing them to take into account the context of recently viewed object sizes. Indeed, these parietal object size responses may depend on the range of object sizes presented (Harvey et al., 2015). By following the range of presented sizes, we speculate that object size processing could represent an object's likely real-world size, and also increase the range of objects whose sizes we could accurately perceive and interact with. Therefore, we hypothesize that these object size selective responses may depend on the context of recent sizes in which an object is viewed. This would increase their effective range and perhaps attract perceived object size towards the likely real-world object size, thereby compensating for the variable relationship to retinal size.

Here we ask whether the sizes of recently presented objects affect object size perception and the representation of object size in human parietal cortex. First, we used psychophysical methods to demonstrate effects of trial history on object size perception. We demonstrated that the perceived size of presented objects was attracted towards both the average object size across all trials (a central tendency effect) and the object size in the previous trial (a serial dependence effect). Second, we determined the object size preferences of neural populations in the posterior parietal object size map using two different ranges of object sizes. We find that increasing presented object sizes considerably increases object size preferences and tuning widths. As with perceived object sizes, neural object size preferences were attracted towards the sizes of recently presented objects. Such a context-dependent perception and neural representation of object size may compensate for changes in retinal size with distance and increase the range of object sizes that can be perceived and represented.

2. Materials and methods

2.1. Subjects

We present behavioral data from five subjects (two male, age range 18–34 years). We present fMRI data from four different subjects (all male, age range 25–40 years). All were well educated, with good mathematical abilities. All had normal or corrected to normal visual acuity. All experimental procedures were cleared by the ethics committee of University Medical Center Utrecht.

2.2. Psychophysics stimuli

We presented psychophysics stimuli on a 40 × 32 cm Sony Trinitron CPD-E500E CRT monitor. The subjects viewed the display from a distance of 75 cm. Display resolution was 1280 × 1024 pixels and frame rate was 75 Hz.

The stimuli (Fig. 1) were generated in Matlab using the PsychToolbox (Brainard, 1997). A large diagonal cross, composed of thin red lines, crossed the entire display, a design that facilitates accurate fixation. Subjects were asked to fixate the intersection of the cross. In each trial, a black filled circle was presented on gray background. The circle's position was randomized, but constrained so that it fell entirely within the central 1.5° (radius) of the visual field. There were 15 possible circle sizes, linearly spaced between 0.06° and 2.8° diameter. The circle was displayed for 320 ms, followed by a white noise mask for 320 ms. A white outlined circle then appeared, with a random initial size within the same range and centered on the fixation cross in the center of the display. Subjects changed the size of this response circle to reproduce

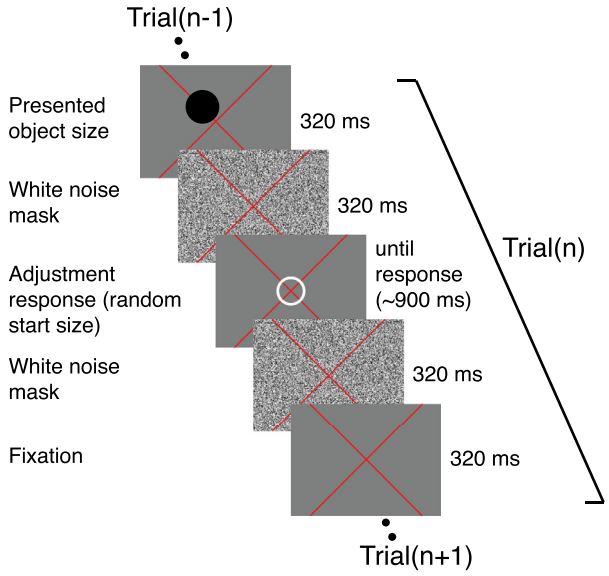

Fig. 1. Psychophysics experimental procedure. We began each trial by presenting a black filled circle of random size, randomly positioned within 1.5° of the center of the fixation cross. After 320 ms, this display was backward-masked with white noise for a further 320 ms. This is followed by a response display consisting of a white outline circle, centered at fixation, beginning at a random size. The subject then attempted to reproduce the size of the initial black circle using horizontal computer mouse movements and clicking when they perceived the matched size. This typically took around 900 ms. The response display was then backward-masked for 320 ms with white noise, before showing a 320 ms gray display and the beginning of the next trial. A red fixation cross over the whole screen was shown throughout, immediately behind the circles.

the size of the black circle they had just seen by moving a computer mouse left and right, clicking the mouse when they perceived the sizes to match. A white noise mask was then displayed for 320ms, followed by a 320ms inter-stimulus interval, followed by the next trial.

Following recent experiments on serial dependence (Fischer and Whitney, 2014), we hypothesized that the perceived and reproduced size of the circle should be attracted to the size of the circle presented on the previous trial. We tested 15 sizes, evenly distributed from 0.05° to 1.4° radius. We generated a pseudo-random sequence of trials for each subject where each circle size was preceded by every other circle size five times. We split these trials into five test sessions, of about 15 minutes each. The first trial of each session was random for the first session and then presented the same size as the last trial of the previous session. The response to the first trial of each session was not analyzed as there was no previous trial. This made 1130 total trials per subject (15 possible sizes of current trial × 15 possible sizes of previous trial + 5 initial trials of each session).

To demonstrate that perceived size was attracted to the size in the previous trial, rather than responses being attracted to responses in previous trials, subjects did not give a response for one of these five trial pairs, randomly distributed throughout the trial sequence (Fischer and Whitney, 2014). In these no-response trials, no response circle was presented, and the display remained blank for the subject's average response time over previous trials, before a mask was shown and the next trial began. We can therefore demonstrate that the response to the second of these trials was attracted to the size shown in the first, even though no response was given for the first trial.

2.3. Psychophysics analysis

For each trial, we calculated the difference between the presented object size and the object size reproduced by the subject, the response error. The slope of the relationship between this response error and the

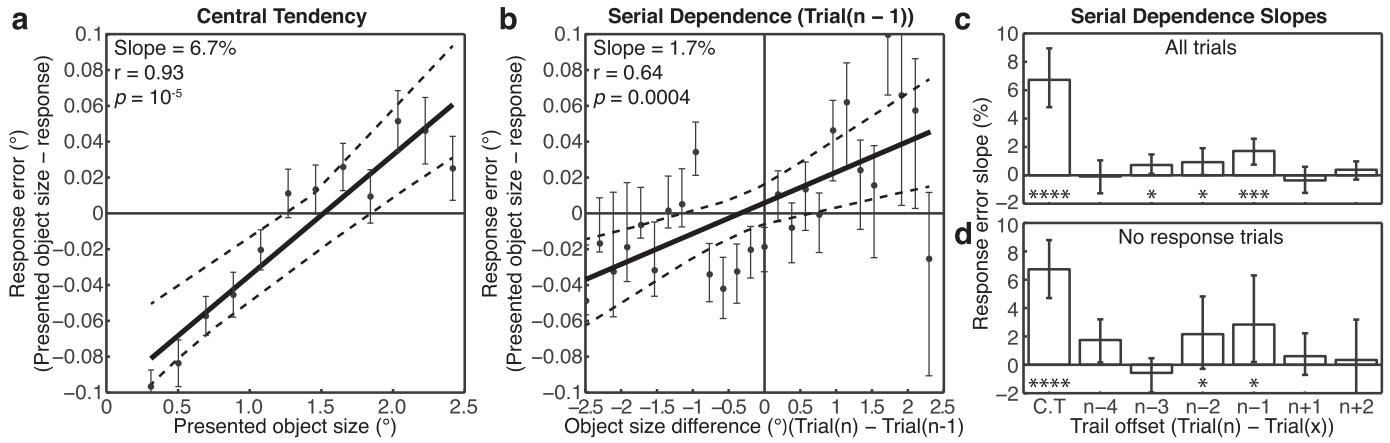

Fig. 2. Effects of trial history on perceived object size. (a) Perceived object size on the current trial is attracted towards the average object size over all trials (1.4°), a central tendency or regression to the mean effect. Response error is therefore significantly correlated with presented object size. (b) Perceived object size was also attracted towards the object size presented on the previous trial, after subtracting the central tendency effect. Response error is therefore significantly correlated with the difference in object size between the current trial (trial(n)) and the previous trial (trial(n – 1)). Circles are the mean response error across all trials with the same object size (A, n=12) or trial difference (B, n=26), and the correlations are conducted on these means. Solid line is the best fit, dashed lines are the 95% confidence intervals of the fit (determined by bootstrapping). (c) The slope of the response error is affected by trial offset, with trial(n – 1), trial(n – 2) and trial(n – 3) all contributing to the response error on trial(n). These trials have smaller effects than the central tendency (C.T.). Future trials do not have an effect. (d) This serial dependence effect is also significant in the fewer trails where no response was given on trial(n – 1) and trial(n – 2). Error bars show the 95% confidence interval of the slope, determined by bootstrapping. Significance of the correlations: * p<0.05, *** p=0.0004, **** p=10^{-5}.

presented object size quantifies the magnitude of the central tendency, i.e. the attraction of the perceived size to the average presented size across all trials.

To examine serial dependence effects, we must first account for this central tendency. Because all object sizes are equally likely to be preceded by all other sizes, a large object is likely to be preceded by a smaller object. So, both central tendency and serial dependence effects predict that a large object's size will be underestimated. But a serial dependence predicts a larger underestimation than that predicted by the central tendency if the previous trial's object size is smaller than the average object size.

We first quantify the central tendency by fitting the linear relationship between the mean response error for each presented object size (grouped across all subjects and trials, i.e. the points shown in Fig. 2A) and the object size. We determine the statistical significance of this relationship using Pearson's correlation between these values. To quantify the serial dependence, we then take response error from the each trial and subtract the response error predicted by the central tendency for that size (which is independent of the previous trial's object size). We then examine the relationship between the resulting adjusted response error and the difference between current and previous object sizes, the trial difference. Again, we grouped this across all subjects and trials (i.e. the points shown in Fig. 2B). We determined the correlation between the trial difference and response error using Pearson's correlation because a simple linear function described the observed relationship well. We also calculated the trial difference between the presented object size and the object size presented further in the past (to examine the time course of effects) or in the future (a control against statistical artefacts (Cicchini et al., 2014)). We also repeat this analysis using only trials presented after no-response trials to demonstrate that serial dependence effects did not rely on attraction of responses over consecutive trials.

We excluded trials where presented object sizes were below 0.25° radius. Subjects could not respond that the object size was less than zero, so for very small object sizes subjects were likely to respond that the presented object was larger than it was. In most trials with very small object sizes, the average trial's object size and the previous trial's object size were larger than current object sizes, so this lower response limit at zero size is likely to artificially introduce the expected relationship between response error and both presented object size and trial difference.

2.4. FMRI stimuli

We presented fMRI stimuli by back-projection onto a 15.0 × 7.9 cm screen inside the MRI bore. The subject viewed the display through prisms and mirrors, and the total distance from the subject's eyes (in the scanner) to the display screen was 41 cm, giving a vertical size of 11° visual angle. Visible display resolution was 1024 × 538 pixels.

The stimuli were generated in Matlab using the PsychToolbox (Brainard, 1997). A large diagonal cross, composed of thin red lines, crossed the entire display, a design that facilitates accurate fixation. Subjects were asked to fixate the intersection of the cross. We compare responses to two different stimulus configurations: one contained small object sizes, while the other contained larger object sizes. The small object size configuration consisted of single objects (circles) with diameters of 0.06–1.4° presented entirely within the central 0.75° (radius) of the visual field. In the large object size configuration, all of these dimensions doubled. Circles had diameters of 0.12–2.8° presented entirely within the central 1.5° (radius) of the visual field. As such, both object size and spacing differed between stimulus configurations to produce different contexts of visual dimensions.

Presenting these circles in a small central stimulus area decreased the need to make eye movements to view the circles. It also minimized the cortical surface extent of the visually responsive part of the brain activated by presentation of the stimulus, avoiding confusion between spatially tuned responses and object size-tuned responses.

Circles were randomly positioned at each presentation so that each circle fell entirely within the central 0.75° (small object sizes configuration) or 1.5° (large objects sizes configuration). Each of the many presentations (384 presentations for each object size in each stimulus configuration) contained circles placed in a new, random position. Averaging these responses to different visual positions minimized links between particular visual field positions and particular object sizes (Harvey et al., 2013).

All stimuli were presented as black filled circles on a gray background. Circles were presented briefly (300 ms). This was repeated ev-

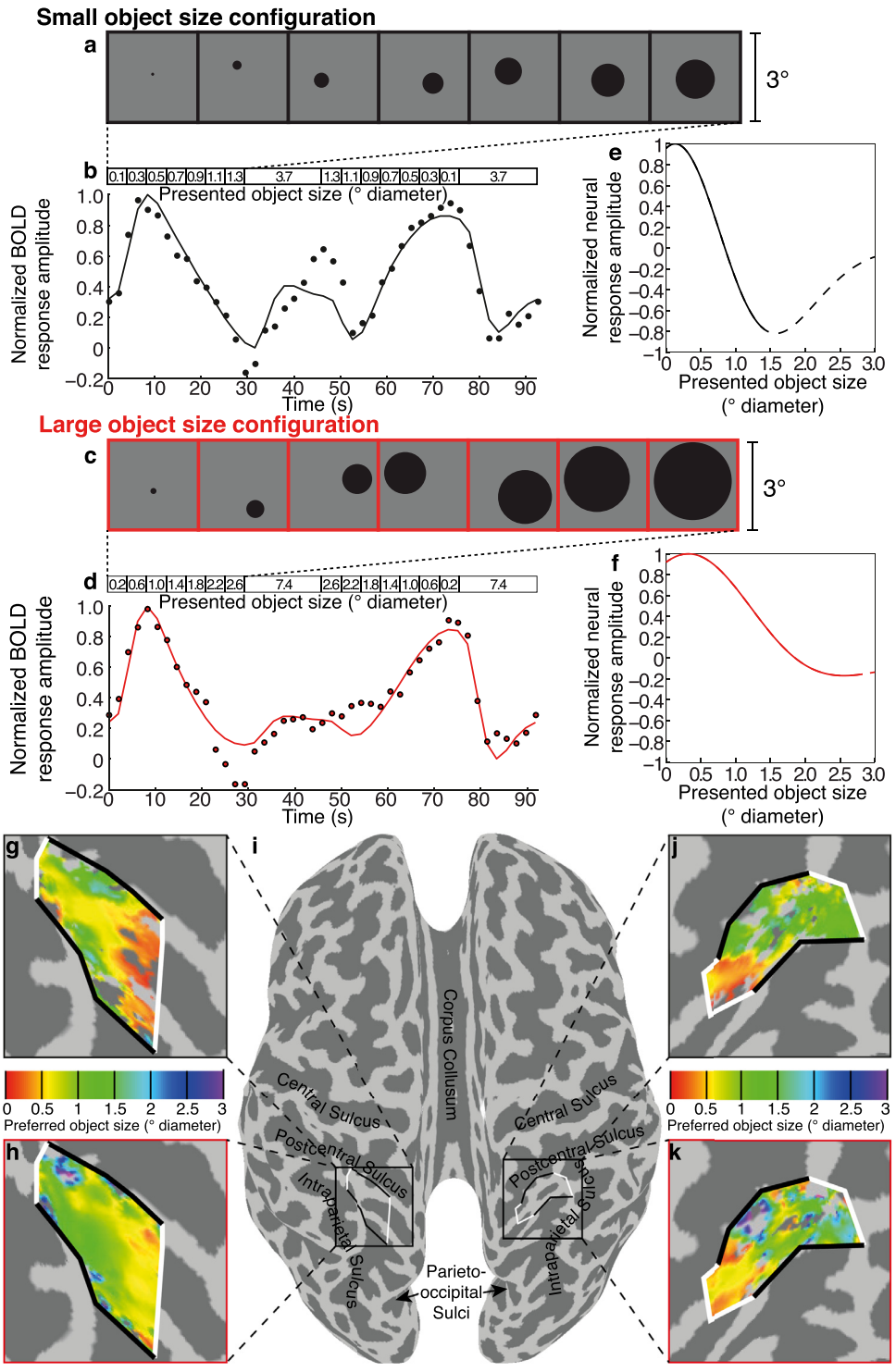

Fig. 3. Effects of stimulus object size range on fMRI responses. (a & c) We presented stimuli that varied in object size over time. We compared two stimulus configurations, a small object size configuration (diameters 0.06–1.4°, a) and a large object size configuration (diameters 0.12–2.8°, c). (b & d) FMRI BOLD responses evoked by these different stimulus sequences at the same example recording site. Despite the large difference in presented object sizes, responses were relatively similar. Dots show the response amplitude at each time point. (e & f) We summarize these responses to the stimulus sequence using pRF neural response models, whose predictions are shown by the lines in (b) and (d). The best fitting neural response functions differ considerably between stimulus configurations. Dashed lines show predictions of responses outside the presented stimulus range, which were not measured. (g, h, j, k) For both stimulus configurations, the preferred object sizes of individual recording sites gradually progress across the surface of the parietal object size map. However, the preferred object size of the same recording sites was larger when measured using the large object size configuration. (i) The posterior parietal cortical location of the maps shown in (g, h, j, k).

ery 700 ms, each time with a new random location presented, with 400 ms presentation of a uniform gray background between circle presentations. This was repeated three times, over 2100 ms (1 TR, fMRI volume acquisition), before the size changed. On 10% of the presentations, the circles were shown in white instead of black. Subjects were instructed to press a button when this happened to ensure they were paying attention to the circles during fMRI acquisition. No object size judgments were required. Subjects responded on 80–100% of white circle presentations within each scanning run.

Circles with diameters of 0.06° to 1.4° (small object sizes configuration, Fig. 3a) or 0.12° to 2.8° (large object sizes configuration, Fig. 3c) were shown as the main stimulus, first presented in linearly increasing order. This was followed by a longer period (16.8 s) where the circle was 3.7° (small object sizes configuration) or 7.4° (large object sizes configuration) in diameter, followed by the same object sizes in descending order, followed by another long period of 3.7° or 7.4° diameter circles. This sequence was repeated four times in each scanning run. The centers of these largest circles were randomly placed, but they reached larger maximum eccentricities, 2.6° and 5.2° respectively, covering a large part

of the visual field. These long periods showing this largest circle had a similar function to the blank periods used in visual field mapping stimuli in population receptive field experiments, allowing us to distinguish between very small and very large tuning widths, i.e. between populations which responded at all times and those that never responded (Dumoulin and Wandell, 2008; Harvey et al., 2013). During this period, little neural response was expected from neurons with small preferred object sizes because such a large object size should be well outside of the range that elicits strong responses. This allows hemodynamic responses to return back to baseline between blocks of changing object size. However, using large objects (rather than no objects) provides a stronger visual stimulus than the other stimuli. As such, neural populations responding to the contrast energy of the stimulus should respond most strongly during presentation of large circles, avoiding confusion with populations preferring a specific large object size.

Stimuli were presented three times between changes, ensuring strong fMRI responses and facilitating measurements of response preferences. As in many fMRI experiments, these stimuli likely cause some adaptation to the presented object sizes (Burr and Ross, 2008; Piazza et al., 2011). We aim to minimize effects of adaptation on tuning estimates by modeling responses to stimuli with both ascending and descending changes. We thus counterbalance adaptation effects by presenting stimuli that give both higher and lower responses before presentation of any object size. As the neural response model must fit both of these response sequences with one set of tuning parameters, the resulting tuning parameters reflect the preferred stimulus without strong dependence on preceding stimuli.

2.5. MRI acquisition and preprocessing

We acquired fMRI data on a 7T Philips Achieva 7T scanner. Acquisition and preprocessing protocols are described in full in Harvey et al. (2015). Briefly, we acquired T1-weighted anatomical scans, automatically segmented these with Freesurfer, then manually edited labels to minimize segmentation errors using ITK-SNAP. This provided a highly accurate model of the cortical surface at the gray-white matter border for analysis of cortical organization. We acquired T2*-weighted functional images on a Philips 7T scanner using a 32 channel head coil at a resolution of $1.77 \times 1.77 \times 1.75$ mm, with 41 interleaved slices. TR was 2100 ms, TE was 25 ms, and flip angle was 70 degrees. Functional runs were each 176 time frames (369.6 s) in duration. Eight repeated runs were acquired within the same session for each stimulus configuration. Responses to each stimulus configuration were acquired on different days.

FMRI analysis was performed using Vistasoft, which is freely available at (https://github.com/vistalab/vistasoft). We first measured and corrected for head movement and motion artifacts between and within functional scans. We aligned functional data from each scanning session to anatomical scans and interpolated them into the anatomical segmentation space. We averaged responses to each stimulus configuration together. We fit separate models to each configuration's data.

2.6. fMRI data-analysis

Object size tuned neural response models were estimated from the fMRI data and stimulus time course, as previously described (Harvey et al., 2015). This approach is based on methods we developed to estimate visuo-spatial population receptive field properties in human visual cortex (Dumoulin and Wandell, 2008).

Population receptive field models describe the aggregate tuning of the neural population within each fMRI recording site. A forward model predicts neural responses at each time point depending on which stimulus was shown. The models describe tuning to object size using Gaussian functions characterized by: (1) a preferred object size (mean of the Gaussian distribution); (2) a tuning width (standard deviation of the Gaussian); (3) an inhibitory surround width (standard deviation of a negative Gaussian with the same mean). Inclusion of an inhibitory surround follows recent demonstrations of surround inhibition in object size selective responses (Harvey et al., 2015). By examining the overlap of the stimulus at each time point with this tuning model, a prediction of the neuronal response time course is generated. By convolving this with a hemodynamic response function (HRF), a predicted fMRI time course is generated. The predicted fMRI time courses were generated for all combinations of a large range of candidate preferred object size, tuning width, and inhibitory surround width parameters. For each recording point, the parameters were chosen from the prediction that fit the data most closely by minimizing the sum of squared errors (R^2, variance explained) between the predicted and observed fMRI time series. To convert these R^2 to probabilities of observing these model fits by chance, we generated a null distribution by fitting tuning models to recordings from 191,000 white matter recording points in the same scans. We then determine the proportion of fits exceeding any particular R^2. We correct these probabilities for multiple comparisons using false discovery rate correction (Chumbley et al., 2010), taking all gray matter voxels in the scanning volume into account.

The candidate preferred object sizes extend beyond the range shown, allowing model fit parameters beyond this range. This allows us to be confident that returned parameters within the stimulus range are reported accurately, rather than the best fit of a limited set. However, recording points with preferences modeled outside the stimulus range must be treated with caution. In such recording points, response amplitude monotonically increases or decreases across the stimulus range. As such we have little confidence that the preferred tuning estimate is correct here, so these recording points were not labeled on cortical surface renderings and were excluded from further analyses.

We estimate the HRF parameters across the whole acquired fMRI volume from the data, using a near-identical procedure we employ in visual cortex (Harvey and Dumoulin, 2011). Briefly, by having the stimulus pass through the stimulus range in both ascending and descending directions, we can derive the HRF properties. We estimated the HRF parameters by comparing predicted and measured time-series and chose the HRF parameters that minimized the difference between prediction and measurements over the entire volume for each stimulus configuration. Next, we averaged the HRF parameters determined from each configuration's data and used those HRF parameters to re-estimate the tuning models. This procedure improved the goodness of fit and ensured the same HRF is used in modeling responses to all configurations and at every point in the brain. Very similar results, though with less good model fits, were obtained by fitting the data using a canonical HRF (Friston et al., 1998), again analogous to results we have obtained in visual cortex (Harvey and Dumoulin, 2011).

2.7. ROI definitions

We focus on the area around the previously defined object size map in the posterior parietal cortex (Harvey et al., 2013).

We first rendered the preferred object sizes of each recording site on the cortical surface. From this, we define our object size map ROI. Medial and lateral borders of the ROI (the 'ends') each followed lines of equal preferred object size at the low and high ends, respectively, of the preferred object size range seen in each stimulus configuration. Anterior and posterior borders (the 'sides') describe the edges of the topographic organization, which coincided with decreases in the goodness of model fits. We repeated this procedure for both small and large object size stimulus configurations. The resulting ROIs coincided closely in the two stimulus configurations, so we defined a single ROI across both stimulus configurations including only recording sites that lay in both ROIs. Lines of highest and lowest preferred object size were very similar in both cases. We excluded from the ROI any recording sites that: 1) did not have at least 30% variance explained by the object size tuning models for both stimulus configurations; or 2) had an object size preference outside the stimulus range in object size tuning models for either

stimulus configuration. This ensured the same recording sites were used for both stimulus configurations.

2.8. Comparisons between tuning models

To determine whether neural tuning changed between stimulus configurations, we first compared the predictive accuracy of separate tuning models fit to each stimulus configuration against a single tuning model fit to both configurations. Here we split our repeated scanning runs into two halves of odd or even scans and, for each half, fit both separate and single tuning models. To evaluate the fits of these models, we quantified the variance each model explained in the fMRI signal from the complementary half of scans. This split-scans cross-validation approach allows us to compare the goodness of fit of different models, without biases that would arise from additional free parameters when fitting separate tuning models: these models will only achieve better fits when the difference between models captures repeatable signals.

To determine whether tuning for visual field positions presented in our stimuli contributed to the responses to our object size stimuli, we first determined the cumulative positions of the object bodies and their edges shown for each presented object size. We then used these as inputs to conventional visual field position-tuned pRF models to predict the responses to the visual field positions covered by the stimuli. For each of the resulting pRF models, we compared the variance explained by each model to the variance explained by object size tuning in the same cross-validation split.

2.9. Analysis of changes across the ROI

Having defined lines following the lowest and highest preferred object sizes seen in each map ROI, we then calculated the distance along the cortical surface from each point in each ROI to the nearest point on each of these lines. The ratio between the distances to each 'end' line gives a normalized distance along the ROI in the primary direction of change of object size preferences. We multiplied this normalized distance by the mean length of the ROI in this direction.

For every 2 mm increase in distance along the ROI, we formed a bin of recording sites, then calculated the mean and standard error of the preferred object sizes of the sites within the bin for each stimulus configuration. To compare preferred object sizes between stimulus configurations, we performed a paired samples t-test of the difference between the mean preferred object sizes in each of these cortical distance bins.

2.10. Tuning widths

To determine how tuning width changed with preferred object size, we followed the procedure previously used to examine relationships between preferred numerosity and tuning width (Harvey et al., 2013). For each recording site within the map ROI, we first reconstructed the difference of Gaussian (DoG) function describing the relationship between presented object size and response amplitude. We measured the width of this function at half its maximum amplitude, the full width at half maximum (FWHM), and used this measure of tuning width as it includes contributions of both positive and negative response.

We aimed to compare tuning widths between stimulus configurations. However, because preferred object sizes of the recording sites change with stimulus configuration, we make two comparisons. First, we compare tuning widths of the same groups of recordings sites to test whether these also change. As for comparisons of preferred numerosities at the same recording sites, we formed a bin of recording sites for every 2 mm increase in distance along the ROI. We calculated the mean and standard error of the object size tuning widths of the sites within the bin for each stimulus configuration. To compare object size tuning width between stimulus configurations, we performed a paired samples t-test of the difference between the mean object size tuning widths in each of these cortical distance bins.

Second, we compare tuning widths of different groups of recordings sites with the same preferred object sizes. Here, we formed a bin of recording sites for every 0.1° increase in preferred object size. We calculated the mean and standard error of the object size tuning widths of the sites within the bin for each stimulus configuration. To compare object size tuning width between stimulus configurations, we performed a paired samples t-test of the difference between the mean object size tuning widths in each of these preferred object size bins. We limited this analysis to preferred object sizes below 1.4° because these fell within the stimulus range for both stimulus configurations. Where the ROI did not contain recording sites with preferred object sizes over this whole range, comparisons were limited to the range of preferred object sizes seen in both stimulus configurations.

Fig. 5 shows a set of example tuning functions for a range of preferred object sizes. To produce these tuning functions, we took tuning model parameters of all recording points in all hemispheres, specifically the widths and amplitudes of the best fitting positive and negative (suppressive) Gaussian tuning functions. For each of these parameters, we took the best fitting cumulative Gaussian sigmoid functions, which describe how that parameter changes with preferred object size. We then evaluated these fit lines for preferred object sizes within the stimulus range and used the resulting parameters to plot the example tuning functions shown.

2.11. Data and code availability

The code generated during this study is available in the Vistasoft repository (https://github.com/vistalab/vistasoft).

The datasets supporting the current study have not yet been deposited in a public repository because of issues regarding public sharing of medical images under the EU's General Data Protection Regulation. They are available from the corresponding author on request.

3. Results

3.1. Psychophysics

3.1.1. Central tendency of size perception

We analyzed how the object sizes presented in previous trials affect the difference between the presented object size and perceived object size (i.e. how trial history affects response errors). We found both a central tendency effect (or regression to the mean) and a smaller serial dependence effect. First, the response error was correlated with the presented object size (Fig. 2a). When objects were smaller than the mean object size, their size was overestimated. When objects were larger than the mean object size, their size was underestimated. As the object size moved further from the mean, the absolute response error increased. This is consistent with a central tendency, where perceived object size is attracted towards the mean object size. The response error was 6.7% of the difference between the presented object size and the mean object size.

3.1.2. Serial dependence of size perception

All object sizes were preceded equally frequently by all other object sizes. Therefore, a trial with a large object size is more likely to be preceded by a smaller object than a larger object. To account for this, we subtracted the response error predicted by the central tendency from the response error on every trial before looking for effects of previous trials. This revealed a serial dependence effect: the perceived object size was significantly attracted towards the object size presented on the previous trial (Fig. 2b). The response bias was on average 1.7% of the difference between the presented object size and the object size presented in the previous trial. Earlier trials also had a significant effect on responses: Perceived object size was attracted to the object size presented two and three trails back, with mean bias of 0.9% and 0.7% of the trial difference respectively (Fig. 2c). We also tested for attraction to the object sizes

presented on future trails, a strong control against statistical artefacts (Cicchini et al., 2014), and found no effect. These serial dependence effects are considerably smaller than the central tendency effect, and less statistically significant.

In one fifth of trials we did not present a response display. This allowed us to distinguish between perception being attracted to perception of previous trails or responses being attracted to responses of previous trials. If we examine response errors in the same way, but using only trials where no response was given on previous trails, we again find significant attraction of responses to the object size presented on previous trials (Fig. 2d). This effect was only significant for the previous trial and two trials back.

4. Functional MRI

Here, we presented two stimulus configurations that differed in the size and spacing of presented objects. In the first (small object sizes configuration), we presented small object sizes (0.06–1.4° diameter circles) in a small area of the central visual field (1.5° diameter) (Fig. 3a). In the second (large object sizes configuration), we presented larger object sizes (0.12–2.8° diameter circles) in a larger area of the central visual field (3.0° diameter) (Fig. 3c). As such, the large object sizes configuration had double the object sizes and spacing of the small object sizes configuration.

4.1. Tuned responses to object size

As demonstrated previously (Harvey et al., 2015), when we showed a stimulus sequence with systematic changes in object size we find responses in the parietal cortex that increase at specific times in the stimulus sequence (Fig. 3b & 3d). Despite the large difference in presented object sizes at each time point, the time course of responses to these stimuli at the same recording site were relatively similar. Using object size-selective population receptive field (pRF) models, we summarize the different fMRI responses for our two stimulus configurations (Fig. 3e–f). We fit object size tuning as linear DoG functions that include below-baseline suppressive surround responses (Harvey et al., 2015). These object size tuning models summarize the fMRI responses seen using three parameters: (i) preferred object size, (ii) tuning width, and (iii) width of the suppressive surround. They explained the recorded responses well in both stimulus configurations (Small object sizes configuration: mean $r^2 = 0.52$, median $r^2 = 0.51$, mean $p = 0.014$, false discovery rate (FDR) corrected. Large object sizes configuration: mean $r^2 = 0.46$, median $r^2 = 0.44$, mean $p = 0.018$) in the posterior parietal object size map. These tuning functions differ considerably between stimulus configurations.

These tuned responses to object size predict responses to our stimuli significantly better than their pRF's responses to the visual field positions of the stimuli (t=6.51, p=0.0003, n=8 hemispheres). We use a cross-validation approach to demonstrate that the extra response variance explained by separate models is repeatable and does not result from overfitting of non-repeatable responses.

4.2. Responses differ between stimulus configurations

To determine whether responses to our two stimulus configurations differ, we first ask whether a single tuning model fit to both stimulus configurations can capture responses as well as separate tuning models for each stimulus configuration. We find that separate tuning models fit to each stimulus configuration capture responses to both stimulus configurations significantly better than a single tuning model (t=4.02, p=0.005, n=8) in cross-validated data.

4.3. Topographic maps of preferred object size

We projected each recording site's preferred object size onto the cortical surface in the posterior parietal cortex, around the previously defined object size map (see Materials and Methods). This revealed orderly topographic maps of object size preferences at the same location in both object size stimulus configurations (Fig. 3g–h), but the preferred object sizes of the same recording sites were considerably larger when determined using responses to the large object size configuration.

To quantify this organization, we sorted recording sites by their cortical distance from same lines of minimum and maximum object sizes preferences found, which coincided closely in both stimulus configurations. We plotted preferred object size against this distance for each configuration (Fig. 4a). For both stimulus configurations we took the average preferred object sizes of all recording sites within every 2mm progression along the combined map ROI. Only recording sites that lay in the object size maps derived from both stimulus configurations were included in the final object size map ROI, so we compare the same groups of recording sites in both stimulus configurations. Preferred object size consistently increases significantly across both hemispheres' cortical surfaces in both stimulus configurations (Permutation test. Small object size configuration: p<0.006 in every hemisphere, p<0.0001 in all hemispheres combined. Large object size configuration: p<0.02 in seven of eight hemispheres, no significant difference in one hemisphere, p<0.0001 in all hemispheres combined).

4.4. Parietal object size preferences follow the stimulus range

Preferred object sizes within these maps differed considerably between stimulus configurations. For each hemisphere's object size map ROI, we compared the preferred object sizes of all recording sites within the map between stimulus configurations using Wilcoxon's signed rank test. The same recording sites preferred significantly larger object sizes in the large object size configuration than the small object size configuration in every subject and hemisphere (p<0.003 in every hemisphere, $p<10^{-20}$ in all hemispheres combined). However, although the presented objects were double the size in the large than the small object size configuration, preferred object sizes in the large object size configuration were often significantly less than double those in the small object size configuration (p<0.0004 in five of eight hemispheres, no significant difference in three hemispheres, $p<10^{-16}$ in all hemispheres combined).

4.5. Changes in tuning width with cortical distance and preferred object size

We have previously found that object size tuning widths decrease as preferred object sizes increase in the small object size configuration (Harvey et al., 2015). Because preferred object sizes increase across the cortical surface, tuning widths consistently decrease significantly across both hemispheres' cortical surfaces in this configuration (Fig. 4b) (p<0.03 in seven of eight hemispheres, no significant difference in one hemisphere, p<0.0001 in all hemispheres combined). However, in the large object size configuration, there was no consistent change in tuning widths with cortical distance.

We captured the change in tuning widths with preferred object size using a cumulative Gaussian sigmoid function (Fig. 4c). For the large object size configuration, a sigmoid function captured tuning width changes significantly better than a linear function (p=0.0012 in all hemispheres combined, cross-validated), though sigmoid and linear functions fit similarly well for the small object size configuration. Regardless of the function used, tuning widths decrease significantly with increasing preferred object size (Linear fits with permutation tests: Both object size configurations p<0.00001. Sigmoid fits with nonlinear cross-validation confidence interval tests (Seber and Wild, 1989): Small object size configuration p=0.0056, Large object size configuration p=0.000004).

4.6. Parietal object size tuning widths follow the stimulus range

As preferred object size differed between configurations, we made two comparisons of tuning width between stimulus configurations. First, do tuning widths differ at the same recording sites? Second, do tuning

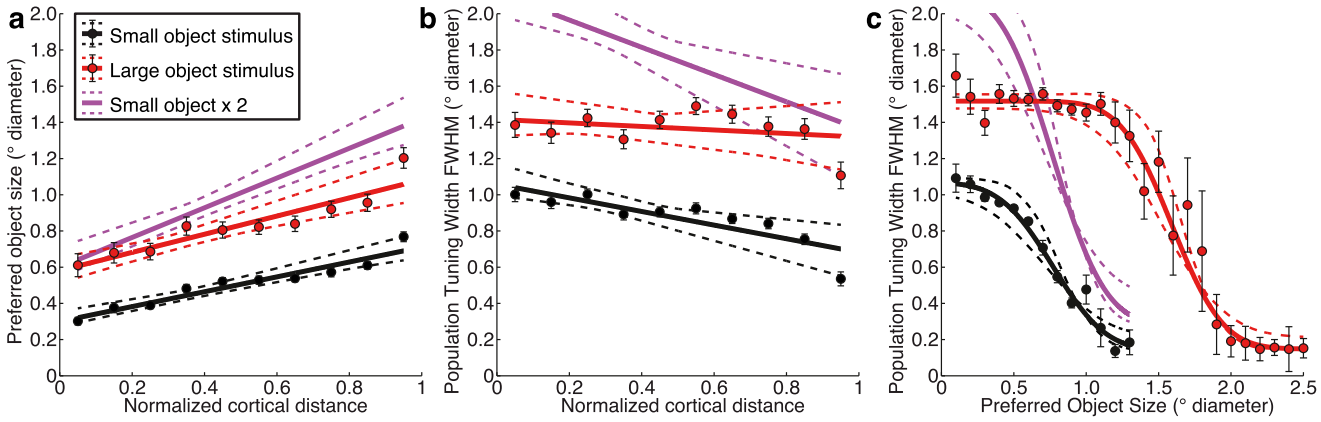

Fig. 4. Comparison of preferred object sizes and tuning widths measured with large and small object size configurations. (a) In both stimulus configurations, the preferred object size increased significantly with distance along the object size map. However, preferred object sizes at the same locations were significantly larger when measured using the large object size configuration than when using the small object size configuration. Although the large object size configuration consisted of objects with double the size of those in the small object size configuration, preferred object sizes in the large object size configuration were significantly smaller than double those in the small object size configuration, so did not scale completely with the difference in object size. (b) At the same recording sites, tuning widths of object size response functions were also significantly larger in the large object size configuration, but significantly smaller than double, those in the small object size configuration. (c) In both stimulus configurations, tuning widths decreased significantly with preferred object size, particularly when approaching the maximum of the presented object size range, following a sigmoid function. In different recording sites with matched preferred object sizes, tuning widths were significantly larger in the large object size configuration. Tuning widths in the large object size configuration were not significantly different from double those in the small object size configuration. However, these two functions have very different slopes so the tuning widths in the large object size configuration are again not double those in the small object size configuration.

widths differ at different recording sites with matched preferred object sizes?

The same recording sites preferred significantly larger object sizes in the large object size configuration than the small object size configuration (Fig. 4b) ($p<0.003$ in seven of eight hemispheres, no significant difference in one hemisphere, $p<10^{-20}$ in all hemispheres combined). However, again, object size tuning widths in the large object size configuration were significantly less than twice those in the small object size configuration ($p<0.01$ in every hemisphere, $p=10^{-20}$ in all hemispheres combined).

To compare object size tuning widths at different recording sites with matched preferred object sizes, we first took the average tuning width of all recording sites within every 0.1° interval of preferred object size (Fig. 4c). Bins of recording sites with the same preferred object sizes had significantly larger object size tuning widths in the large object size configuration than the small object size configuration in all subjects and hemispheres ($p<0.04$ in all eight hemispheres, $p=0.0002$ in all hemispheres combined). Object size tuning widths in the large object size configuration were not significantly different from double those in the small object size configuration in any hemisphere. However, these two functions had very different slopes (Fig. 4c), so a straightforward doubling of tuning widths from the small object size configuration captures the tuning widths from the large object size configuration poorly.

4.7. Parietal object size tuning functions adapt to the presented range

Plotting the range of response functions from the different stimulus configurations (Fig. 5) revealed how the entire neural population in the parietal object size map responds. For both stimulus configurations, these response functions narrowed as the stimulus approaches the maximum presented size. As a result, response functions with a range of preferred object sizes converged on zero response amplitude at the maximum presented object size (as previously shown for the small object size configuration (Harvey et al., 2015)). The response of the entire map therefore represented the range of recently presented stimuli as well as the size of the current stimulus.

For the small object size configuration, tuning functions over the entire presented range converged at this maximum size, while for the large object size configuration only the tuning functions with preferred object size above approximately 1.2° diameter do so. This suggests that neural populations in recording sites with smaller preferred object sizes may have reached a maximum tuning width here, while those with preferred object sizes above 1.2° diameter may continue to follow further increases in the presented object size range. For both stimulus configurations, we found very few recording sites with preferred object sizes near the maximum presented size, suggesting these object sizes may be encoded in response functions with smaller preferred object sizes.

5. Discussion

We find that object size perception is attracted towards both the average size of recently presented objects (a central tendency effect) and towards the size of objects presented in immediately preceding trials (a serial dependence effect, which is smaller). Similarly, object size preferences and object size tuning widths of neural populations within the parietal object size map are larger when responding to larger objects than when responding to smaller objects. However, neither the preferred object sizes or tuning widths increase in proportion to the increase in object size. These properties change together to cover the range of presented object sizes. Therefore, perception and neural responses to object size are both influenced by the temporal context of sizes in which an object is seen.

5.1. Adaptation, serial dependence and central tendency

Our results show that both perception and neural response preferences for object size follow the context of recently presented sizes. On the surface, these results appear to mimic classic adaptation effects. However, in classical adaptation effects (Blakemore and Sutton, 1969; Burr and Ross, 2008), repeated stimulus presentation causes neural responses to the adapted stimulus state to decrease, repelling perception of subsequent stimuli from the adapted stimulus state. Such adaptation effects would repel object size perception and tuning away from recent

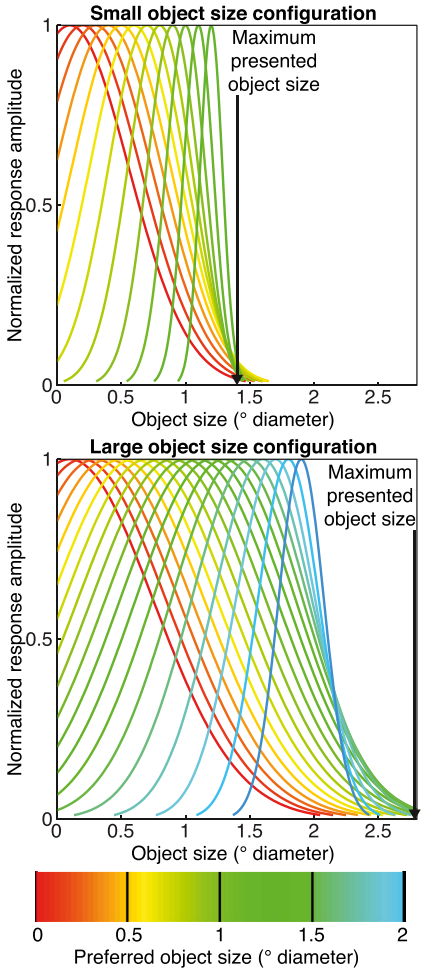

Fig. 5. Neural population response functions follow the range of presented object sizes. For both stimulus configurations, average response functions with a range of preferred object sizes (colors) converge on zero response amplitude at the maximum presented object size. The response of the entire map therefore represented the range of recently presented stimuli as well as the size of the current stimulus.

stimulus states, contrary to our results. We also did not present the same stimulus state repeatedly, the object size was always changing. Therefore, we believe that classical adaptation effects cannot explain our results.

On the other hand, recent reports describe serial dependence effects operating at shorter time scales, where stimulus perception is attracted towards recent stimulus states (Cicchini et al., 2014; Fischer and Whitney, 2014; Liberman et al., 2014). This is consistent with our results. Perceptual serial dependence has been described before in numerosity perception (Cicchini et al., 2014), whose perceptual and neural representation are closely linked to object size (Harvey et al., 2015; Hurewitz et al., 2006; Tudusciuc and Nieder, 2007). These serial dependence effects are proposed to improve perceptual accuracy when stimuli are not changing state, by using previous stimulus states as a Bayesian prior to the current stimulus state (Cicchini et al., 2014).

Central tendency effects operate at an intermediate time scale. They attract perceived object size towards the average of all previously presented object sizes. The central tendency effect we observe is larger than the sum of serial dependence effects over trials n − 1 to n − 3, so may be distinct from the serial dependence effect we observe. Nevertheless, the direction of central tendency and serial dependence effects is the same, and we cannot distinguish between these effects at the time scale of our fMRI experiment. Therefore, we propose that the effects of stimulus range on neural object size preferences may underlie either or both of these perceptual effects.

The sizes of the psychophysical serial dependence and central tendency effects are small (1.7% and 6.7% respectively of the subject's object size judgements), while the preferred object sizes of our recording sites change much more (increasing by over 50% from small to large object size configurations). However, we would expect such small effects given our psychophysics experiment's setup. Subjects gave the perceived size of the object by changing the size of a circle to match the size they just saw. We expected the perceived size of the response circle, not only the test circle, to be affected by previous stimuli. The perceived size of the test circle should be affected more than the response circle because: 1) The test circle was presented first, closer in time to previous stimuli; 2) The response circle (white outline) did not share visual features with the previous test stimuli (black filled circle), a strategy used by previous serial dependence experiments to affect the test stimulus more than the response stimulus (Fischer and Whitney, 2014). As we expect the perceived size of both the test circle and the response circle to be affected, we cannot straightforwardly estimate the magnitude of change in test circle size perception.

This psychophysics experiment was designed to efficiently test for effects of temporal context on size perception. In the fMRI experiment circles were presented repeatedly and rapidly, changing in size gradually. As a result, the presented circle sizes are predictable, so we cannot ask subjects to make a behavioral judgement of object size (even outside the scanner): they can predict the correct answer here. These designs suit their respective experiments, but are very different, precluding straightforward comparison.

5.2. Mechanisms of object size tuning and context dependence

Several mechanisms might produce responses like those we report. Here we examine possible interpretations of our findings.

Could object size tuning in both stimulus configurations reflect responses to another feature of the stimulus that co-varies with object size? Here, several features change when we change object sizes: display luminance, spatial frequency, object diameter, radius and circumference. We have previously demonstrated that display luminance changes do not produce similar responses (Harvey et al., 2015). Diameter, radius, circumference and fundamental spatial frequency are directly proportional to each other in the circles we use, so tuning to any of these features predicts identical responses. We do not believe this distinction is important, as all of these are measures of retinal size. However, responses to any of these retinal stimulus dimensions should not change with object size context. Therefore, it is possible that our fMRI responses might reflect the likely real-world size of the object and separate this from its retinal size, though the functional consequences of the observed changes in object size selectivity and their link to changes in object size perception require further experiments to support this possibility.

Could object size tuning reflect receptive field position selectivity of these neural populations, or the extent of eye movements? We presented the circles in a small central stimulus area to minimize the extent of eye movements and the extent of the stimulated area of cortex. By limiting circles to fall entirely within this area, the average change in position between sequential presentations (so the eccentricity that would be stimulated if subjects were looking at the first circle's position when a new circle appeared) varies slightly with object size. We set up the fMRI stimulus to minimize this possibility by asking subjects to fixate a central cross and leaving time between the earlier circle's disappearance and the later circle's appearance. We are confident that the observed responses do not reflect the change in position (either of the eyes or the stimulated eccentricity) because we previously included a control condition where the change in position of sequentially presented circles was held constant, and we still found object size tuning (Harvey et al., 2015).

There is also a possibility that object size tuning might effectively reflect pRF size. The object size producing the largest response might simply be that which stimulates the pRF's excitatory center but not its suppressive surround (Zuiderbaan et al., 2012). As pRF sizes increase with visual field map eccentricity, this might confuse visual field maps with object size maps. However, we have previously used visual field mapping to show that object size preferences of our recording sites were not correlated with pRF eccentricity or size in the visual field maps with which they overlap (Harvey et al., 2015). Furthermore, the pRF sizes of these recording sites is far larger than the presented object sizes.

We previously proposed that object size-tuned responses could be derived from visuo-spatial tuning through mechanisms that associate outputs of visuo-spatially tuned populations with similar receptive field sizes, regardless of preferred visual field position preferences. The contextual effects we describe here may argue against such a mechanism. However, close links between object size selective populations and particular receptive field sizes could be affected by context if receptive field sizes were strongly dependent on presented object sizes. Visual receptive field sizes are affected by low-level visual features (Dumoulin et al., 2014; Harvey and Dumoulin, 2016). Object size context may similarly affect visual receptive field sizes, which could affect object size tuning derived from these receptive field sizes.

Alternatively, object size-selective responses could be derived from inputs with a broad range of receptive field sizes. This would allow context-dependent selectivity to arise during the derivation of object size tuning, as these inputs could be weighted depending on the range of presented object sizes.

So, effects of size context seem unlikely to arise in early visual areas where visual spatial representations are closely tied to retinal input. Rather, context is likely to affect response preferences either in later visuo-spatial responses, which are more context-dependent, or after object size selectivity is derived from visuo-spatial responses (Murray et al., 2006). These late stage effects are consistent with previously described properties of visual serial dependence, such as broad retinotopic spread and a dependence on attention (Fischer and Whitney, 2014). Classical adaptation effects, on the other hand, are retinotopically limited, suggesting they may depend more on early visual areas. This late stage object size representation may be fed back to early visual cortex to affect its representation of the object's spatial extent (Murray et al., 2006), but our experimental design does not allow us to investigate the extent of the object's visual field map representation.

The effects we describe demonstrate that the response preferences within object size maps can be flexible and are not invariant to stimulus context. This may be surprising because topographic maps are generally seen as invariant. The structure of primary sensory topographic maps (retinotopic, tonotopic and somatotopic maps) is fixed and invariant because it reflects the fixed structure of their connections to their respective sensory organs. However, at least in retinotopic maps, the neural response selectivity in these maps is not fixed. Even in V1, position selectivity is affected by contextual factors like spatial attention (Klein et al., 2014), visual motion (Whitney et al., 2003; Harvey & Dumoulin, 2016) and apparent distance (Murray et al., 2006). We see similar effects here: size preferences are context-dependent but change across the map similarly for both size ranges.

5.3. Implications for size perception

The context-dependence we observe in the perception and neural representation of object size could facilitate size constancy: the systematic underestimation of changes in object size. By taking into account the range of recently viewed retinal sizes, the brain's representation and the subject's perception of object size could follow the likely real-world size of an object. This could compensate for the variable relationship between retinal and real-world sizes. This would facilitate interactions with our environment, for example by allowing us to choose the correct grip aperture to fit the object's real-world size. Nevertheless, it is important to highlight that the functional consequences of the observed changes in object size selectivity and their link to changes in object size perception require further experiments to support this possibility.

The primary factor in the relationship between retinal and real-world object size is object distance. Humans use several cues to determine object distance, including binocular disparity, oculomotor cues (accommodation and vergence) and image cues like object size and perspective. Here, we do not manipulate binocular disparity or oculomotor cues, so we can exclude these changes from our context-dependent effects. While changes in distance are often linked to changes in binocular disparity, object size itself provides a strong cue to distance, often predicting perceived distance better than disparity does (Rushton and Wann, 1999). We can easily perceive distance in flat images, such as televisions screens and photographs, where image cues for distance are separated from binocular disparity and oculomotor cues. And we can perceive distance monocularly, where binocular disparity and vergence are eliminated. Size constancy is equally strong for binocular and monocular presentations (Holway and Boring, 1941). Object size perception is strongly influenced by the spatial context of nearby object sizes and spatial frequencies, for example in the Ponzo illusion or the Ames room. Our results suggest that temporal object size context may similarly influence size perception.

More generally, context-dependence in quantity processing systems may allow quantity cognition to react flexibly to the context of quantities in our environment at a given time. This would increase the efficiency of neural coding and reduce noise here by exploiting temporal redundancies in natural scenes: the tendency for visual features to remain similar over time (Burr and Cicchini, 2014; Cicchini et al., 2014; Fischer and Whitney, 2014). Alternatively, context-dependence may increase the range of quantities that a neural system can represent: a context-dependent system can vary the range of sizes it represents, increasing the range of sizes it can represent.

6. Conclusions

Real-world object size helps guide human behavior and decisions, but its computation is confounded by the variable relationship between retinal size and real-world size. Size constancy biases object size estimates to stay constant when retinal size changes, as real-world size does. Our perception and neural representation of object size follows the history of presented object sizes, which may enable parietal processing of object size to more accurately represent likely real-world size. This may enable multisensory parietal processing of spatial dimensions to plan actions more accurately by following real-world size rather than retinal size.

Author contributions

Conceptualization, SD, JA, BH; Methodology, SK, AF and BH; Software, SK and BH; Validation, SK and BH; Formal analysis, SK and BH; Investigation, SK, AF and BH; Data curation, SK, AF and BH; Writing - original draft, SK and BH; Writing - review and editing, SK, AF, SD, JA and BH; Visualization, SK and BH; Supervision, SD, JA and BH; Project administration, BH; Funding acquisition, SD, JA and BH.

Acknowledgments

This work was supported by Netherlands Organization for Scientific Research grants #452.17.012 to BH, #016.Vici.185.050 to SD, by Portuguese Foundation for Science and Technology Investgador grant #IF/01405/2014 to BH and Programa COMPETE grant #PTDC/MHC-PCN/0522/2014 to JA and SK, by Royal Netherlands Academy of Arts and Sciences Ammodo award to SD and by Biotechnology and Biological Sciences Research Council (UK) grant #BB/S006605/1 to AF, and by an European Research Council Starting Grant (#802553, "ContentMAP") to JA.

References

Blakemore, C., Sutton, P., 1969. Size adaptation: a new aftereffect. Science 166, 245–247.

Brainard, D.H., 1997. The psychophysics toolbox. Spat. Vis. 10, 433–436.

Burr, D., Cicchini, G.M., 2014. Vision: efficient adaptive coding. Curr. Biol. 24, R1096–R1098.

Burr, D., Ross, J., 2008. A visual sense of number. Curr. Biol. 18, 425–428.

Chumbley, J., Worsley, K., Flandin, G., Friston, K., 2010. Topological FDR for neuroimaging. Neuroimage 49, 3057–3064.

Cicchini, G.M., Anobile, G., Burr, D.C., 2014. Compressive mapping of number to space reflects dynamic encoding mechanisms, not static logarithmic transform. Proc. Natl. Acad. Sci. USA 111, 7867–7872.

Dumoulin, S.O., Hess, R.F., May, K.A., Harvey, B.M., Rokers, B., Barendregt, M., 2014. Contour extracting networks in early extrastriate cortex. J. Vis. 14, 18.

Dumoulin, S.O., Wandell, B.A., 2008. Population receptive field estimates in human visual cortex. Neuroimage 39, 647–660.

Ferri, S., Rizzolatti, G., Orban, G.A., 2015. The organization of the posterior parietal cortex devoted to upper limb actions: an fMRI study. Hum. Brain Mapp. 36, 3845–3866.

Fischer, J., Whitney, D., 2014. Serial dependence in visual perception. Nat. Neurosci. 17, 738–743.

Friston, K.J., Fletcher, P., Josephs, O., Holmes, A., Rugg, M.D., Turner, R., 1998. Event-related fMRI: characterizing differential responses. Neuroimage 7, 30–40.

Harvey, B.M., Dumoulin, S.O., 2011. The relationship between cortical magnification factor and population receptive field size in human visual cortex: constancies in cortical architecture. J. Neurosci. 31, 13604–13612.

Harvey, B.M., Dumoulin, S.O., 2016. Visual motion transforms visual space representations similarly throughout the human visual hierarchy. Neuroimage 127, 173–185.

Harvey, B.M., Fracasso, A., Petridou, N., Dumoulin, S.O., 2015. Topographic representations of object size and relationships with numerosity reveal generalized quantity processing in human parietal cortex. Proc. Natl. Acad. Sci. USA 112, 13525–13530.

Harvey, B.M., Klein, B.P., Petridou, N., Dumoulin, S.O., 2013. Topographic representation of numerosity in the human parietal cortex. Science 341, 1123–1126.

Holway, A.H., Boring, E.G., 1941. Determinants of apparent visual size with distance variant. Am. J. Psychol. 54, 21–37.

Hurewitz, F., Gelman, R., Schnitzer, B., 2006. Sometimes area counts more than number. Proc. Natl. Acad. Sci. USA 103, 19599–19604.

Klein, B.P., Harvey, B.M., Dumoulin, S.O., 2014. Attraction of position preference by spatial attention throughout human visual cortex. Neuron 84, 227–237.

Liberman, A., Fischer, J., Whitney, D., 2014. Serial dependence in the perception of faces. Curr. Biol. 24, 2569–2574.

Murray, S.O., Boyaci, H., Kersten, D., 2006. The representation of perceived angular size in human primary visual cortex. Nat. Neurosci. 9, 429–434.

Orban, G.A., Caruana, F., 2014. The neural basis of human tool use. Front. Psychol. 5, 310.

Piazza, M., Fumarola, A., Chinello, A., Melcher, D., 2011. Subitizing reflects visuo-spatial object individuation capacity. Cognition 121, 147–153.

Rushton, S.K., Wann, J.P., 1999. Weighted combination of size and disparity: a computational model for timing a ball catch. Nat. Neurosci. 2, 186–190.

Seber, G., Wild, C., 1989. Nonlinear Regression. Wiley, New York 1989.

Silver, M.A., Ress, D., Heeger, D.J., 2005. Topographic maps of visual spatial attention in human parietal cortex. J. Neurophysiol. 94, 1358–1371.

Tudusciuc, O., Nieder, A., 2007. Neuronal population coding of continuous and discrete quantity in the primate posterior parietal cortex. Proc. Natl. Acad. Sci. USA 104, 14513–14518.

Whitney, D, Goltz, HC, Thomas, CG, Gati, JS, Menon, RS, Goodale, MA, 2003. Flexible retinotopy: motion-dependent position coding in the visual cortex. Science 302, 878–881.

Zuiderbaan, W., Harvey, B.M., Dumoulin, S.O., 2012. Modeling center-surround configurations in population receptive fields using fMRI. J. Vis. 12 (3), 10.